FULL PAPER

Hindering the Oxidation of Silicene with Non-Reactive Encapsulation

Alessandro Molle, Carlo Grazianetti, Daniele Chiappe, Eugenio Cinquanta, Elena Cianci, Grazia Tallarida, and Marco Fanciulli*

The chemical stability of buckled silicene, i.e., the silicon counterpart of graphene, is investigated then resulting in a low reactivity with O_2 when dosing up to 1000 L and in a progressive oxidation under ambient conditions. The latter drawback is addressed by engineering ad hoc Al- and Al_2O_3-based encapsulations of the silicene layer. This encapsulation design can be generally applied to any silicene configuration, irrespective of the support substrate, and it leads to the fabrication of atomically sharp and chemically intact Al/silicene and Al_2O_3/silicene interfaces that can be functionally used for ex situ characterization as well as for gated device fabrication.

1. Introduction

Since its up-to-date identification,[1,2] silicene, the silicon counterpart of graphene, has raised a booming appeal as a route to circumvent the gapless character of graphene, which makes it preferable for radio frequency (RF) amplifiers, but not quite suitable to logic switch functionalities.[1] From this point of view, the silicene can be regarded as a promising option for a future ultra-scaled electronics based on newly emerging 2D nanosheets,[4,5] such as MoS_2, GaS, GaSe, etc.[3] At the moment, buckled silicene structures have been experimentally reported on substrates with metallic character, such as Ag, ZrB_2 or Ir.[1,2,7–9] Opposed to the semi-metallic behavior of graphene, the intrinsic buckling of the silicene lattice might confer band-gap opening[1,8] as well as access basic properties such as the spin quantum Hall effect and topologically protected insulating states,[10] or ferromagnetic behavior.[11] Exploring the electronic properties of the silicene either from a fundamental and a technological point of view imposes to integrate silicene in a device-suited configuration. To this scope, interfacing silicene with a gate dielectric material is essential for any feasible voltage bias application but also to save it from possibly destructive reactivity under ambient conditions. While disentangling silicene from a metal template is still an on-going challenge, on-top interface engineering of silicene is addressed here by taking into account two key-issues, the assessment of the chemical stability (especially in air where the graphene is known to be chemically nonreactive) and the development of an nonreactive encapsulation process.

In this study, oxidation of silicene is investigated with O_2 dosing in an ultrahigh vacuum (UHV) environment and upon exposure to air. Second, an Al-based protective encapsulation of silicene is achieved by growing an epitaxial Al film with varying thickness under close in situ monitoring via real time grazing incidence electron diffraction and x-ray photoelectron spectroscopy (XPS). Deposition of the Al capping layer is intended to hinder silicene oxidation in air, then resulting in an intact Al_2O_3/Al/silicene/Ag heterostructure in which the intercalated silicene is not impacted in its lattice features and chemical bonding. Further improvement can be obtained by growing the Al_2O_3 in UHV ambient. Hence, these efforts enabled us to fabricate a chemically stable Al_2O_3/silicene/Ag heterostructure through a carefully tailored co-deposition of Al and O_2 thus paving the way to ex situ characterization and to future device configurations incorporating gated silicene.

2. Experimental Section

Experiments were performed in a molecular beam epitaxy (MBE) system (Omicron Nanotechnology GmbH) equipped with three interconnected chambers for substrate preparation, chemical analysis, and scanning tunnelling microscopy (STM) investigations with a base pressure of 5×10^{-11} mbar. The Ag(111) monocrystal (13×6 mm^2) was cleaned by several cycles of Ar^+ ion sputtering (1 keV) and subsequent annealing (30 min) at 530 °C. Temperature was measured by combining the use of a K-thermocouple placed in proximity of the sample and an external infrared pyrometer. Epitaxial Si was grown on an Ag(111) substrate at 250 °C by depositing Si from a thermally heated crucible and with a rate of 2.3×10^{-2} monolayer (ML)/min. Al was deposited by means of a k-cell

Dr. A. Molle, C. Grazianetti, Dr. D. Chiappe, Dr. E. Cinquanta, Dr. E. Cianci, G. Tallarida, Prof. M. Fanciulli
Laboratorio MDM, IMM-CNR, via C. Olivetti 2, I-20864 Agrate Brianza (MB), Italy
E-mail: alessandro.molle@mdm.imm.cnr.it
C. Grazianetti, Prof. M. Fanciulli
Dipartimento di Scienza dei Materiali
Università degli Studi di Milano Bicocca
via R. Cozzi 53, I-20126, Milano (MI), Italy

DOI: 10.1002/adfm.201300354

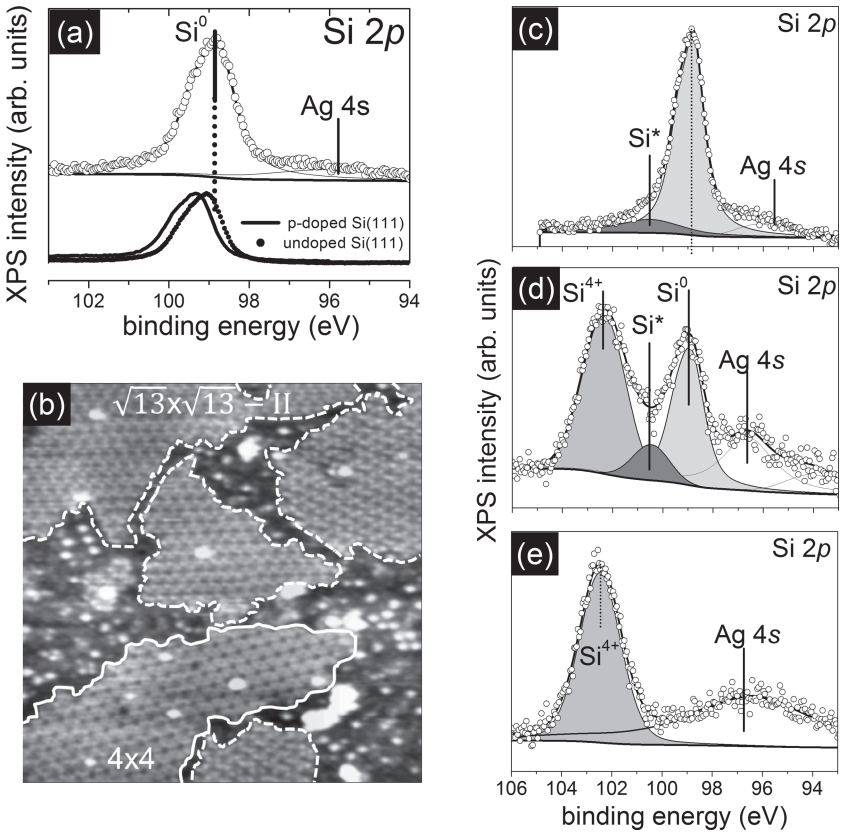

Figure 1. a) Si 2p XPS line of silicene epitaxially grown on Ag(111) (top panel) and of reference substrates of p-doped Si(111) (black line) and nominally undoped Si(111) (black dots) monocrystals. b) 35 × 35 nm^2 STM topography (tip bias –2 V, tunneling current 0.2 nA) illustrating the interplay of differently structured silicene domains. 4 × 4 and $(\sqrt{3}+\sqrt{3})$ superstructures are respectively framed by full and dashed contour lines; Si 2p XPS line of silicene exposed to 1000 L (c); to air for 3 min (d); to air for one day (e).

(MBE-Komponenten) with Al deposition rate ranging from 3.0 to 0.1 Å/min and O_2 was supplied through an ultrapure O_2 line. A structural check was performed by in situ reflection high energy (30 keV) electron diffraction (RHEED) monitoring in real time with the growth. Silicene topography was probed by in situ scanning tunneling microscopy (STM) with a tip voltage of –2 V and a tunneling current of 0.2 nA. In situ XPS measurements were performed by means of a non-monochromatic (Mg Kα) X-ray source and a semispherical analyser working with pass energy of 20 eV and a variable take-off angle (from 37° to 70° from the sample surface plane). Fit to the XPS lines involved Shirley background removal and decomposition in pseudo Voigt functions (products of Gaussians and Lorentzians). Doublets of Voigt functions were adopted when treating p core levels. Ex situ Raman scattering characterization was performed by using a Renishaw Invia spectrometer equipped with the 2.5 eV/488 nm line of an Ar^+ laser line focused on the sample by a 50× 0.75 N.A. Leica objective providing a spot diameter of about 0.8 μm. The power at the sample was maintained at 1 mW in order to prevent laser-induced sample heating. Hundreds of spectra were acquired in order to obtain the highest signal/noise ratio. All the measurements were carried out in a z backscattering geometry.

3. Silicene Oxidation

An atomically resolved topography of the epitaxial silicene on Ag(111) substrates is illustrated in the STM image in **Figure 1**b where differently structured domains can be observed. Evidence of domains reflects the intimate multi-phase character of the silicene layer which is dictated by the details of the buckled bonding disposition.[7,12–14] From a closer inspection, the domains turned out to be prevailingly composed of 4 × 4 and $(\sqrt{3}+\sqrt{3})$-type II superstructures, consistently with the assignment of ref. [14] From in situ XPS monitoring, the Si 2p line related to elemental silicene is peaked at a binding energy (BE) of 98.8 eV and can be well-distinguished from the nearby Ag 4s line from the substrate (see Figure 1a, top panel). The peak positioning is shifted to slightly lower BE compared to the reported Si 2p lines of a p-doped and nominally undoped Si(111) substrates (see Figure 1a, bottom panel for comparison). This fact can be attributed either to an n-type character of silicene (intrinsic of the deposition process) or to an electron transfer from Ag to silicene orbitals. Despite buckling can be related to the intimate matching of the Si wetting layer with the Ag(111) substrate, no substrate induced change in the chemical bonding state of the silicene layer, e.g., Si-Ag bonding, can be deduced from the deconvolution of the Si 2p line in relation with those of a pure Si(111) substrate. The Si 2p line of the silicene exposed to 1000 L of ultrapure O_2 (1 L = 1 s at 1 × 10^{-6} Torr) is reported in Figure 1c. The shape profile of the Si 2p lines exhibits a small asymmetry, which can be related to a minor Si-O component in the proposed peak deconvolution with a chemical shift of 1.5 eV from the elemental silicene peak (see Figure 1a). The scarce oxidation degree is consistent with the reported low reactivity of silicene nanoribbons[15] and can be tentatively related to oxidative pathways through structural defects or domain boundaries that intimately qualify the 2D arrangement of the silicene layer (see Figure 1b and ref. [7]).

A dramatic change in the silicene composition can be deduced already after 3 min exposure to air as documented by the Si 2p line in Figure 1d. The double-peak shape profile of the Si 2p line can be decomposed in three contributions, respectively coming from the elemental bonding of the residual silicene and from two different kinds of Si-O bonding components. The major Si-O component is placed at BE = 102.3 eV being consistent with a preferential SiO_2-like chemisorption (Si^{4+} peak in **Figure 2**d), whereas the other component descends from lower valence states of the Si-O bonding (i.e., sub-oxide species, see the Si* peak in Figure 2c,d).[16] It is relevant to notice that silicene-like bonding (denoted as Si^0 in Figure 2d) still persists on the surface composition even after 3 min exposure to air; nonetheless longer exposure time leads

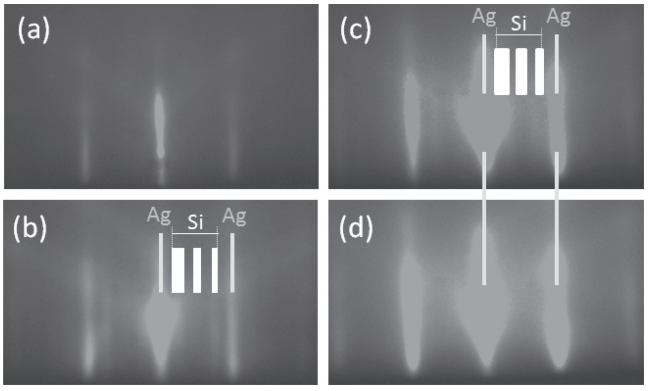

Figure 2. RHEED pattern of a) cleaned Ag(111) surface; b) silicene epitaxially grown on Ag(111) (main streaks indicate the periodicity of the coincidence cell, substreaks are due to the various silicene superstructures, the different width of the substreaks is intended to picture the interplay of different diffraction features arising from non-equivalent silicene superstructures); c) 3-nm-thick Al capping layer on silicene/Ag(111); d) 7-nm-thick Al capping layer on silicene/Ag(111).

to a complete oxidation of the silicene layer in an atomically thin SiO_2 compound (see Figure 1e).

4. Al Encapsulation

Oxidation of silicene in ambient condition represents a serious drawback for any silicene-based device functionalization as well as for a broad range of ex situ probing. As a consequence, encapsulation of the silicene layer is a mandatory task. Capping (at room temperature) with an ultra-thin Al layer emerges as a promising option as the silicene band structure is not significantly altered by alkali metal adatom absorption according to spin-polarized density functional theory calculations.[17] To this purpose, the silicene layer has been capped in situ with a 7-nm-thick MBE-grown Al film at room temperature with an Al growth rate of 3.0 Å/min. To assess Al-induced chemical interaction or structural distortion in the silicene layer, the Al growth has been RHEED monitored in real time and XPS analysis has been performed by taking the Al film thickness as a parameter. Relevant RHEED patterns are reported in Figure 2 for the pristine (1×1) Ag(111) surface (Figure 2a, the as deposited silicene on Ag(111) (Figure 2b) and after 10 min (3 nm, Figure 2c) and 25 min (7 nm, Figure 2d) long Al deposition.

Surface superstructures of the silicon adlayer on Ag(111) can be deduced from the (non-equivalently spaced) sub-streaks of the RHEED pattern in Figure 2b which account for the interplay of the 4×4 and $(\sqrt{3} + \sqrt{3})$ superlattices illustrated in Figure 1b and clearly distinguish the diffraction signatures of silicene domains from the characteristic pattern of the (1×1) Ag(111) surface in Figure 2a. Despite the relatively low deposition temperature, Al proves to grow epitaxial and flat as a well-defined RHEED pattern can be observed during the Al growth and no spotty pattern takes place (see the streaky pattern recorded on a 7-nm-thick Al layer on silicene in Figure 2d). Silicene-related sub-streaks can be still observed after RHEED monitoring up to 10 min long deposition, i.e., 3-nm-thick Al film (see Figure 2b), therein unambiguously indicating the persistence of the silicene arrangement irrespectively of few Al adatom accommodation up to the completion of one Al adlayer. Since the RHEED sub-streaks of extra surface periodicity are usually vanishing in conventionally reconstructed semiconductor surfaces after sub-monolayer adsorption,[18] the latter fact is strikingly indicative of a structurally stable 2D silicene material and of the wetting character of the Al layer. Al-related streaks appear with increasing thickness (see arrows in Figure 2d), which place nearly in correspondence of the pristine Ag(111) streaks as due to the similar unit cell of the Al(111) and the Ag(111) surfaces.

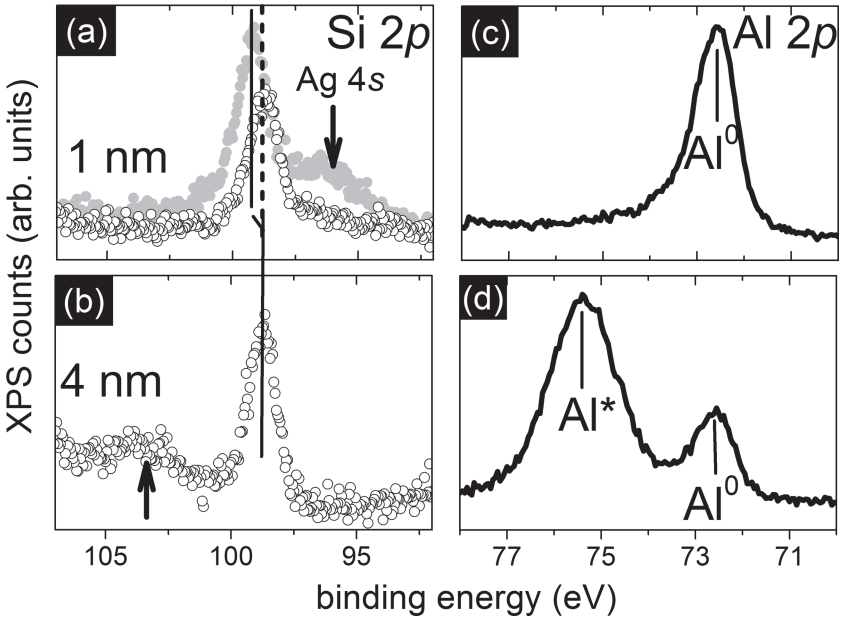

Figure 3. Si 2p XPS line of silicene as a function of the Al capping layer thickness (ϑ): a) ϑ = 1 nm (the reference line of freshly recovered silicene is reported in grey dashed line for comparison); b) $\vartheta = 4$ nm; c) Al 2p line for $\vartheta = 4$ nm indicative of a purely elemental Al-Al bonding of the capping layer; and d) Al 2p line after oxidation of a 7-nm-thick Al capping layer indicative of partial Al oxidation with an Al_2O_3 composition.

In **Figure 3**, XPS probing of the Al 2p and Si 2p lines with increasing Al capping thickness enables us to gain an in situ insight into the compositional depth profiling of the silicene/Al heterostructure in a thickness range compatible with the Si 2p photoelectron mean free path.[19] While the Al 2p line in the inset of Figure 3c is indicative of a purely elemental Al bonding of the capping layer after 1 nm coverage, no change can be detected in the Si 2p lines recorded in 1-nm- and 4-nm-thick Al layer (respectively in Figure 3a,b) with respect to the reference line taken in situ on the as-grown silicene (see grey dots in Figure 3a). A shift of the Si 2p line to lower BE can be observed after Al deposition which can be related to an extra charge exchange between the Al and Si

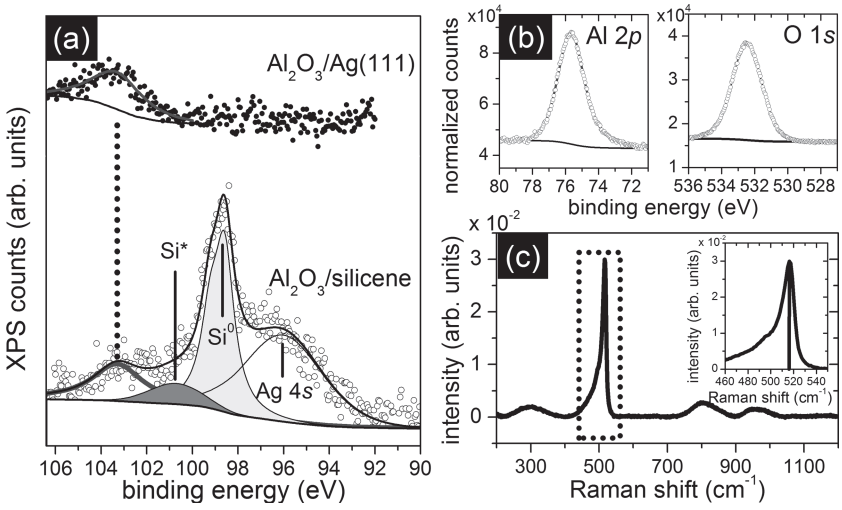

Figure 4. a) Si 2p photoemission line taken after deposition of Al_2O_3 capping layer onto silicene/Ag(111) (bottom) and directly onto the Ag(111) surface for comparison (top). b) Al 2p and O 1s lines with normalized intensity according to the respective atomic sensitivity factors. The areal ratio is consistent with a sesquioxide stoichiometry. c) Ex situ Raman spectrum of the capped sample once exposed to ambient condition. Inset: magnification of the Raman peak related to the silicene nanosheet.

orbitals as much as previously observed in the freshly deposited silicene on Ag. An additional feature can be noticed at BE = 103.5 eV in Figure 3b (see arrow) which is basically Al-related because the same features appears even when Al is directly deposited on Ag(111) without silicene interlayer (see the relevant spectrum in **Figure 4**). Upon exposure of a 7-nm-thick Al capped silicene to air, the Al 2p line in Figure 3d exhibits two components, one (Al^0) related to residual Al-Al bonding at the bottom of the capping layer and one (Al^*) related to partial Al oxidation from the surface level. The chemical shift of the Al^* component amounts to 2.9 eV which corresponds to a major Al_2O_3 composition.[20] Survival of a pure Al layer below the oxidized Al can thus prevent the encapsulated silicene from any possible O_2 chemisorption. The Al_2O_3 formed upon partial Al oxidation exhibits an atomic rms-roughness of 0.33 nm measured by ex situ atomic force microscopy (see Figure SI1, Supporting Information) thus indicating a quite conformal morphology of the Al_2O_3/Al/Si heterostructure on the Ag(111) surface.

5. Al_2O_3 Encapsulation

If the Al_2O_3/Al/silicene configuration can be exploited to access ex situ characterization, engineering an Al_2O_3/silicene interface would be a highly desirable advance for an electronic device oriented dielectric gating. To this purpose, taking benefit from the observed low reactivity of silicene with in situ dosed O_2 (Figure 1), the Al capping layer was deposited in an oxygen overpressure of 10^{-6} Torr (same as used under 1000 L exposure) in order to induce Al_2O_3 formation. In addition, the Al growth rate has been adequately rescaled down to 0.1 Å/min in order to promote the growth of a stoichiometric Al_2O_3 and avoid excess of elemental Al in the adsorbate. According to Figure 3, the bonding states of the Al 2p and Si 2p lines can be regarded as a fingerprint of the physical quality of Al_2O_3/silicene interface and hence of the overall Al_2O_3 encapsulation approach.

The chemical details of the Al_2O_3 encapsulation are scrutinized in Figure 4a,b where, respectively, the Si 2p line is susceptible of any extrinsically induced bonding modification in silicene, and the Al 2p and O 1s line make clear the composition of the oxide capping layer. The Si 2p line can be deconvoluted in four components, namely the Ag 4s line from the Ag substrate, the Si^0 peak indicative of the silicene bonding, and two extra components at BE = 101.6 eV and 103.3 eV, respectively. In agreement with the same feature observed in Figure 3b, the extra-component at BE = 103.3 eV can be definitely assigned to the overlying Al_2O_3 (and unambiguously discriminated from a Si^{4+} bonding state) because the same feature occurs when growing Al_2O_3 directly on Ag(111) (see relevant spectrum in Figure 4a). While the O_2 preferentially reacts with Al, the extra-component at BE = 101.6 eV can be interpreted as the Si^* component in Figure 1c thereby claiming for a limited oxidation of the silicene layer in a sub-stoichiometric valence state. It must be emphasized that the Si 2p line in Figure 4a is largely dominated by the Si^0 elemental bonding component thus proving the nearly complete survival of the silicene layer after Al_2O_3 deposition. This observation is nonetheless consistent with the possible oxidation of highly reactive sites, such as grain boundaries or local defects of silicene (Figure 1b). In addition, quite similarly to the pure Al capping, the Si 2p peak is down-shifted from its pristine BE positioning in the as grown silicene-on-Ag configuration, this fact being either consistent with a charge transfer between the silicene orbitals and the Al_2O_3 ones or with an oxide-induced modification of the electronic state of silicene. Reactive co-deposition of O_2 and Al results in the oxidation of Al in a largely dominant Al^{3+} bonding state placed at BE = 75.6 eV in the Al 2p line and in a O 1s line peaked at BE = 532.5 eV both being univocally indicative of a prevailing Al_2O_3 constitution of the oxide layer (Figure 4, top panels).[18,20] Furthermore, the ratio of the XPS line areas derived from pseudo-Voigt function fit to the spectra and normalized on the relevant atomic sensitivity factors is consistent with a nearly sesquioxide stoichiometry, namely Al and O results in average atomic concentrations of 65% and 35%. Lower Al oxidation states can be deduced from slightly asymmetric low BE tail of the Al 2p line deconvolution in a dramatically minor extent. Ex situ Raman spectroscopy has been performed on the Al_2O_3 capped silicene in order to corroborate the effectiveness of the silicene encapsulation. The Raman spectrum in Figure 4c is largely dominated by a narrow and asymmetric peak at 516 cm^{-1}, which has been shown elsewhere to derive from the honeycomb lattice of the silicene nanosheet.[21] The broad bumps around 300 and 800 cm^{-1} are related to Al_2O_3 bands and the other broad feature at

1000 cm^{-1} can be tentatively assigned to second order Raman scattering from the silicene layer. The signature of the silicene nanosheet in the Raman spectrum of the sample exposed to ambient condition makes further evidence of the effectiveness of the Al_2O_3-based capping process.

6. Conclusions

Based on XPS monitoring of the Si 2p photoemission line, epitaxial silicene grown on Ag(111) proves to be chemically stable upon O_2 exposure up to 1000 L but it undergoes a progressive oxidation in SiO_2 in air. A non-destructive methodology to encapsulate the silicene layer in physically Al_2O_3/Al/silicene/Ag and Al_2O_3/silicene/Ag heterostructures has been demonstrated which makes epitaxial silicene accessible to a broad number of ex situ diagnostic and potentially suitable to gated device configurations. The design of an effective encapsulation layer can be generally applied to any silicene layer regardless of the substrate. The effectiveness of the silicene encapsulation unambiguously resulted from registering the fingerprint of the silicene nanosheet in the ex situ measured Raman spectrum of the Al_2O_3 capped silicene on Ag(111). This can be potentially used as a benchmark to assess the influence of the substrate or to recognize different superstructures in the vibrational properties of silicene.

Supporting Information

Supporting Information is available from the Wiley Online Library or from the author.

Acknowledgements

This research activity was carried out within the framework of the EU project 2D-NANOLATTICES. The project 2D-NANOLATTICE acknowledges the financial support of the Future and Emerging Technologies (FET) programme within the Seventh Framework Programme for Research of the European Commission, under FET-Open grant number: 270749. The authors acknowledge S. Brivio (CNR-IMM) for technical assistance.

Received: January 29, 2013
Revised: February 22, 2013
Published online: April 9, 2013

[1] P. Vogt, P. De Padova, C. Quaresima, J. Avila, E. Frantzeskakis, M. C. Asensio, A. Resta, B. Ealet, G. Le Lay, *Phys. Rev. Lett.* **2012**, *108*, 155501.
[2] C.-L. Lin, R. Arafune, K. Kawahara, N. Tsukahara, E. Minamitani, Y. Kim, N. Takagi, M. Kawai, *Appl. Phys. Express* **2012**, *5*, 045802.
[3] D. J. Late, Bin Liu, H. S. S. Ramakrishna Matte, C. N. R. Rao, V. P. Dravid, *Adv. Funct. Mater.* **2012**, *22*, 1894.
[4] D. J. Late, B. Liu, H. S. S. Ramakrishna Matte, V. P. Dravid, C. N. R. Rao, *ACS Nano* **2012**, *6*, 5635.
[5] D. J. Late, B. Liu, J. Luo, A. Yan, H. S. S. Ramakrishna Matte, M. Grayson, C. N. R. Rao, V. P. Dravid, *Adv. Mater.* **2012**, *24*, 3549.
[6] F. Schwierz, *Nat. Nanotechnol.* **2010**, *5*, 487.
[7] D. Chiappe, C. Grazianetti, G. Tallarida, M. Fanciulli, A. Molle, *Adv. Mater.* **2012**, *24*, 5088.
[8] A. Fleurence, R. Friedlein, T. Ozaki, H. Kawai, Y. Wang, Y. Yamada-Takamura, *Phys. Rev. Lett.* **2012**, *108*, 245501.
[9] L. Meng, Y. Wang, L. Zhang, S. Du, R. Wu, L. Li, Y. Zhang, G. Li, H. Zhou, W. A. Hofer, H.-Jun Gao, *Nano Lett.* **2013**, *13*, 685.
[10] M. Ezawa, *Phys. Rev. Lett.* **2012**, *109*, 055502.
[11] C. W. Zhang, S. S. Yan, *J. Phys. Chem. C* **2012**, *116*, 4163.
[12] B. Feng, Z. Ding, S. Meng, Y. Yao, X. He, P. Cheng, L. Chen, K. Wu, *Nano Lett.* **2012**, *12*, 3507.
[13] D. Jose, A. Datta, *J. Phys. Chem. C* **2012**, *116*, 24639.
[14] H. Jamgotchian, Y. Colignon, N. Hamzaoui, B. Ealet, J. Y. Hoarau, B. Aufray, J. P. Bibérian, *J. Phys.: Condens. Matter* **2012**, *24*, 172001.
[15] P. De Padova, P. Perfetti, B. Olivieri, C. Quaresima, C. Ottaviani, G. Le Lay, *J. Phys.: Condens. Matter* **2012**, *24*, 223001.
[16] F. J. Himpsel, *Phys. Rev. B* **1988**, *38*, 6084.
[17] Xianqing Lin, Jun Ni, *Phys. Rev. B* **2012**, *86*, 075440.
[18] C. Grazianetti, A. Molle, G. Tallarida, S. Spiga, Marco Fanciulli, *J. Phys. Chem. C* **2012**, *116*, 18746.
[19] NIST Standard Reference Database 71, wwws.nist.gov/srd/nist71.cfm (accessed December 2012).
[20] I. Olefjord, H. J. Mathieu, P. Marcus, *Surf. Interface Anal.* **1990**, *15*, 681.
[21] E. Cinquanta, E. Scalise, D. Chiappe, C. Grazianetti, B. Van der Broek, M. Houssa, M. Fanciulli, A. Molle, available online at arXiv:1212.5422.